

Article

Not peer-reviewed version

---

# Safety Profile of *Solanum tuberosum*-Derived Exosomes: Evidence from In Vitro Experiments and Human Skin Tests

---

YeJi Lee , [Radwa Wahid Mohamed](#) <sup>\*</sup> , [Sanghwa Yang](#) <sup>\*</sup>

Posted Date: 20 February 2025

doi: 10.20944/preprints202502.1661.v1

Keywords: *Solanum tuberosum*-derived exosomes (SDE); wound healing; photoaging; inflammation; skin barrier; safety profile



Preprints.org is a free multidisciplinary platform providing preprint service that is dedicated to making early versions of research outputs permanently available and citable. Preprints posted at Preprints.org appear in Web of Science, Crossref, Google Scholar, Scilit, Europe PMC.

Copyright: This open access article is published under a Creative Commons CC BY 4.0 license, which permit the free download, distribution, and reuse, provided that the author and preprint are cited in any reuse.

Article

# Safety Profile of *Solanum tuberosum*-Derived Exosomes: Evidence from *In Vitro* Experiments and Human Skin Tests

Yeji Lee <sup>1</sup>, Radwa Wahid Mohamed <sup>2,\*</sup> and Sanghwa Yang <sup>1,\*</sup>

<sup>1</sup> Research and Development Team, Nextab, Inc., 361, World Cup buk-ro, Mapo-gu, Seoul, 03908, Republic of Korea

<sup>2</sup> Department of Biochemistry and Nutrition, Women's College for Arts, Science and Education, Ain Shams University, Cairo, 11566, Egypt

\* Correspondence: radwa.wahid@women.asu.edu.eg (R.W.M.); admin@nextab.co.kr (S.Y.)

**Abstract:** Repetitive exposure to ultraviolet B (UVB) radiation is known to cause DNA damage and increase levels of reactive oxygen species (ROS), which are linked to the upregulation of matrix metalloproteinases (MMPs) and inflammatory cytokines. These events lead to collagen breakdown by MMPs, resulting in wrinkles, loss of elasticity, and rough, dry skin—typical signs of photoaging—and may even contribute to skin cancers in the long term. We have previously shown that *Solanum tuberosum*-Derived Exosomes (SDE) can repress 80% of the expression of MMP1 and tissue necrosis factor (TNF) at 50 µg/mL without inducing damage to keratinocyte HaCaT cells. In this report, we show that SDEs can be treated to the HaCaT cells up to 1,000 µg/mL without inducing cell death, establishing a safe maximum concentration. SDEs can significantly promote wound healing in a scratch model of wounds in HaCaT cells and elevate the expression of skin barrier genes in HaCaT and fibroblast cell line Detroit 551, which are known to enhance skin cell integrity, prevent water loss, and support natural desquamation. In a skin clinical test including 21 volunteers for 2 weeks, prototypes containing SDEs at 100 µg/mL as the main ingredient significantly enhanced skin elasticity, reduced deep eye wrinkle depth, and decreased melanin content, most importantly, without skin-irritating side effects. These findings suggest that SDEs are a safe, natural complex with antioxidant, anti-inflammatory, and barrier-enhancing effects that can be produced in quantity with relative ease for a potential medical application in humans.

**Keywords:** *Solanum tuberosum*-derived exosomes (SDE); wound healing; photoaging; inflammation; skin barrier; safety profile

## 1. Introduction

Photoaging involves a complex process of DNA damage induced by ultraviolet B (UVB) radiation, which subsequently leads to the induction of matrix metalloproteinase 2 (MMP2) [1]. This process can act synergistically with pathways involving the induction of MMP1, MMP3 and MMP9, which are activated by reactive oxygen species (ROS) generated by UVB exposure [2]. Together, these pathways contribute to the mechanisms underlying wrinkle formation. The skin serves as a crucial protective barrier, performing essential functions such as providing physical, chemical, and biological defenses against environmental threats, preventing water loss, and maintaining permeability. This barrier is primarily upheld by the outermost layer of the epidermis, known as the *stratum corneum* (SC), which relies on the coordinated action of barrier proteins like filaggrin (FLG) [3]. However, external factors such as UVB radiation, wounds and infections continuously impact these vital functions, leading to potential skin damage. One significant consequence of compromised skin barrier function is the development of dermatological conditions such as psoriasis and atopic eczema. In psoriasis, skin barrier damage is characterized by the overexpression of TNF, an

inflammatory cytokine, alongside reduced expression of skin barrier genes, including *FLG* and *loricrin (LOR)* [4]. Evidence suggests that TNF antagonists can promote the re-expression of compromised skin barrier genes, highlighting their therapeutic potential. These agents not only alleviate psoriatic symptoms but also enhance *FLG* and *LOR* expression in human keratinocytes and psoriasis patients *in vivo* [5]. This effectiveness underscores the critical link between TNF, skin barrier integrity, and adverse skin conditions. Moreover, skin wounds caused by burns, injuries, pressure, or friction further compromise the skin barrier. Rapid wound healing is essential for maintaining skin health by preventing dehydration, hypersensitivity, infection, and chronic inflammation [6]. Developing measures that support a healthy skin barrier and accelerate wound healing can significantly reduce social burden and enhance patient quality of life [7].

Exosomes are extracellular vesicles composed of lipid-protein complexes encased in lipid bilayers, typically ranging from 50 to 120 nm in diameter. They are generated by a wide variety of cells from eukaryotic, prokaryotic, and fungal origins. Exosomes convey biomolecules—including mRNA, miRNA, proteins, peptides, DNA, and small natural molecules—to recipient cells *in vitro* and *in vivo*, thereby influencing gene expression [8]. Additionally, exosomes are emerging as promising drug delivery mechanisms for therapeutic agents, including those targeting the brain [9–13]. Among the various sources of exosomes, those derived from plants are particularly noteworthy. These vesicles exhibit physical characteristics like their counterparts from other sources. Plant exosomes offer distinct advantages, evading the immune system when introduced into animals and ensuring high biocompatibility and safety, especially when derived from food plants. Furthermore, lower production costs make plant exosomes a promising option as next-generation carriers for exogenous medicinal agents [14–16]. While extracellular microvesicles share some overlapping anti-inflammatory activities with exosomes, they differ primarily by size, with a mean diameter exceeding 150 nm [17]. Recent significant advances in the cosmetic sector highlight the integration of food and cosmetics by leveraging bioactive substances from edible plants to enhance skin health and beauty [18]. In this context, exosomes derived from consumable plants represent a promising next-generation skincare component due to their efficacy and safety.

Exosomes with a size distribution of 50 to 120 nm in diameter, specifically with a mean diameter of 66 nm, can be isolated from the edible potato (*Solanum tuberosum* L.) using ultracentrifugation [19]. These *Solanum tuberosum*-derived exosomes (SDE) have shown a strong tendency to suppress the expression of *TNF*, an inflammatory cytokine linked to both the initiation and delay of wound healing. Elevated levels of TNF are associated with various dermatological conditions such as psoriasis and atopic dermatitis, where skin barrier function is compromised. By modulating TNF levels, there is potential to support skin barrier integrity and promote wound healing, ultimately contributing to overall skin health [20]. Nanomaterials smaller than 100 nm are particularly interesting in the cosmetic industry, if safety standards are met. Their small size allows them to penetrate deeper into the skin layers, initiating revitalization processes [21]. Given the natural origin and nanoscale properties of SDEs, we investigated their potential effects on skin barrier functions and wound healing. In this study, the impact of SDEs on the expression of key genes associated with skin barrier integrity in human keratinocyte HaCaT cells was evaluated through RT-PCR analyses. We examined the expression of several genes crucial for skin barrier function and hydration: Aquaporin 3 (*AQP3*), a six-transmembrane channel protein, facilitates the transport of water and glycerol, playing a vital role in wound healing and skin barrier maintenance [22,23]. Filaggrin (*FLG*) acts as a filament-aggregating protein, consolidating keratin filaments into dense bundles to enhance the cellular barrier. *FLG* monomers undergo proteolytic degradation into amino acids, which contribute to the synthesis of natural moisturizing factors (NMF), essential for skin hydration, pH regulation, and UV protection [24]. Transglutaminase 1 (*TGM1*), an enzyme with scaffolding properties, aids in creating the cornified envelope by promoting crosslinking among structural proteins, thus enhancing epidermal strength and stability. Mutations that inactivate human *TGM1* disrupt skin barrier function and cornified envelope formation, leading to defects in the stratum corneum. These mutations are associated with lamellar ichthyosis, a condition characterized by

widespread scaling and thickening of the skin [25]. Kallikrein-related peptidase 5 (*KLK5*), a sequence-specific serine protease, is crucial for desquamation, the shedding of corneocytes from the skin surface. This process facilitates epidermal rejuvenation and skin homeostasis while playing a role in preventing skin diseases such as Harlequin Ichthyosis [26–28]. Hyaluronan synthase genes are responsible for producing hyaluronan (hyaluronic acid, HA), a polysaccharide with significant water-binding properties crucial for skin hydration. Exogenous HA supplementation has been shown to enhance skin conditions, including hydration, wrinkle reduction, and increased elasticity [29]. Additionally, nanoparticle-mediated delivery of hyaluronan synthase type 2 (*HAS2*) enzyme elevates endogenous high molecular weight hyaluronic acid and aids in the repair of bone defects in animal models [30]. *HAS3* in the epidermis has been identified as a critical regulator of hyaluronan synthesis [31]. Additionally, to elucidate the role of exosomes in wound healing processes, we evaluated the relative wound closure in HaCaT cells treated with SDEs. Subsequently, we conducted a clinical skin test to evaluate the safety of SDEs on human skin and their effectiveness in reducing deep eye wrinkles and improving overall skin quality.

## 2. Results

### 2.1. Profile of Isolated SDEs

Isolated SDEs were assessed for their integrity and purity. Dynamic light scattering (DLS) analyses of 3 independent exosome preparations confirmed a mean diameter of 66 nm with a standard deviation of 0.74 nm, consistent with previous findings (Figure 1A). No other molecules or contaminants larger than the exosome peak was observed, indicating a purity exceeding 98%. Transmission electron microscopy (TEM) showed that the SDEs exhibit double-layered oval morphologies, confirming that the isolated particles are exosomes (Figure 1B). To assess the prospective use of SDEs in cosmetic applications for human skin, two safety experiments were conducted. First, when the extracted exosomes were cultured on bacterial growth plates for up to 48 h, no contaminating bacterial growth was observed. In contrast, positive control studies demonstrated normal growth of *Candida albicans* on YPD plates and *Staphylococcus epidermidis* BRD on TSA plates. Similarly, *E. coli* DH5 $\alpha$  exhibited standard growth on both LB and MH agar plates, confirming the absence of bacterial contamination during the manufacturing process (Figure 1C). Subsequently, an LD<sub>50</sub> test was performed to determine the maximum safe concentration of SDEs. HaCaT cells were treated with SDEs at concentrations ranging from 1 to 1,000  $\mu\text{g}/\text{mL}$  (Figure 1D). Notably, an initial cell growth-promoting effect was observed at a concentration of 50  $\mu\text{g}/\text{mL}$ , which continued up to 500  $\mu\text{g}/\text{mL}$ . At a concentration of 1,000  $\mu\text{g}/\text{mL}$ , cell growth exhibited a modest 4% reduction relative to the untreated control group, but was not a significant change, suggesting that the maximum safety threshold may extend beyond 1,000  $\mu\text{g}/\text{mL}$  *in vitro*. Therefore, a complete LD<sub>50</sub> dataset was not obtained in this experiment. These findings verify the quality control measures taken in SDE production for human skin applications and demonstrate the inherent safety profile of SDEs

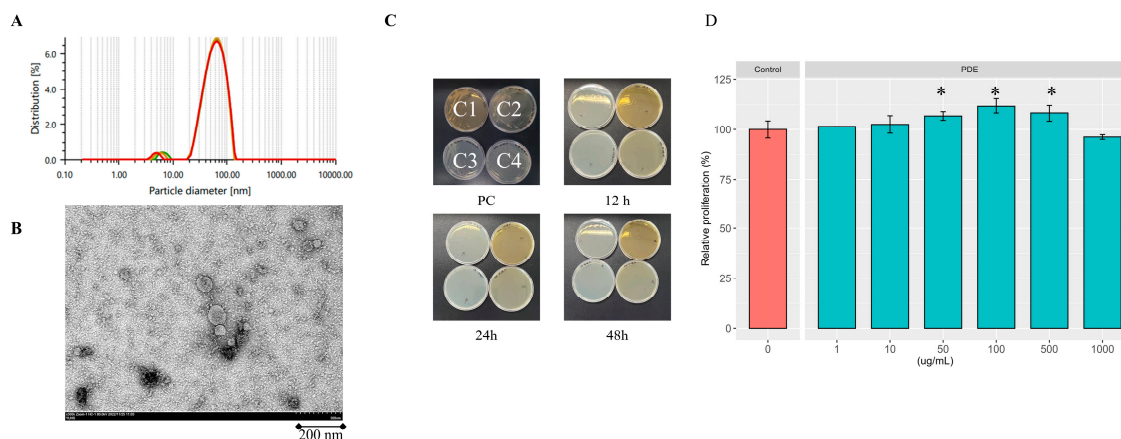


**Figure 1.** Extraction of SDEs and assessment of toxicity. (A) Size assessment of isolated exosomes via dynamic light scattering (DLS). DLS studies were conducted on three independent exosome isolations. (B) Exosome morphology examined via Transmission Electron Microscopy (TEM). (C) Contamination assessments of exosomes. Positive controls (PC) included plating *Candida albicans* on YPD (Yeast Extract Peptone Dextrose) agar plates (C1), *Staphylococcus epidermidis* BRD on TSA (Tryptic Soy Agar) plates (C2), and *Escherichia coli* DH5 $\alpha$  was cultured on LB plates (C3) and Mueller Hinton Agar (MHA) plates for a duration of 48 h (C4). The panels of ExoP\_12h, ExoP\_24h, and ExoP\_48h illustrate the incubation of potato-derived exosomes on YPD, TSA, LB, and MHA plates for durations of 12, 24, and 48 h, respectively. (D) Tests were conducted to determine the lethal concentration of 50 (LC50) on HaCaT cells by administering exosomes at concentrations ranging from 1 to 1,000  $\mu$ g/mL. 'SDEs' refer to *Solanum tuberosum*-derived exosomes.

## 2.2. Impact of SDEs on HaCaT Keratinocyte Wound Healing

HaCaT cells are widely recognized as a standard model *in vitro* keratinocyte for studying inflammatory cytokines and wound healing processes. In this study, we assessed the impact of SDEs on the growth-promoting activities of HaCaT keratinocytes through wound healing experiments. To evaluate the potential effects of SDEs on these cells, artificial wounds were created by gently scratching the cell monolayer. Following this, the cells were treated with either 1X PBS (designated as 'Control') or SDEs in 1X PBS at equivalent volumes. The alterations in the wounds were observed at specified intervals post-treatment (Figure 2A). After measuring the injured regions (Figure 2B) and comparing the percentages of wound closure at 48 h post-treatment, we found that SDE treatment significantly enhanced percentage of wound closure compared with the natural wound closure occurring in the HaCaT cells without SDE treatment (Figure 2C). These results suggest that SDEs may have therapeutic potential in promoting skin repair processes.

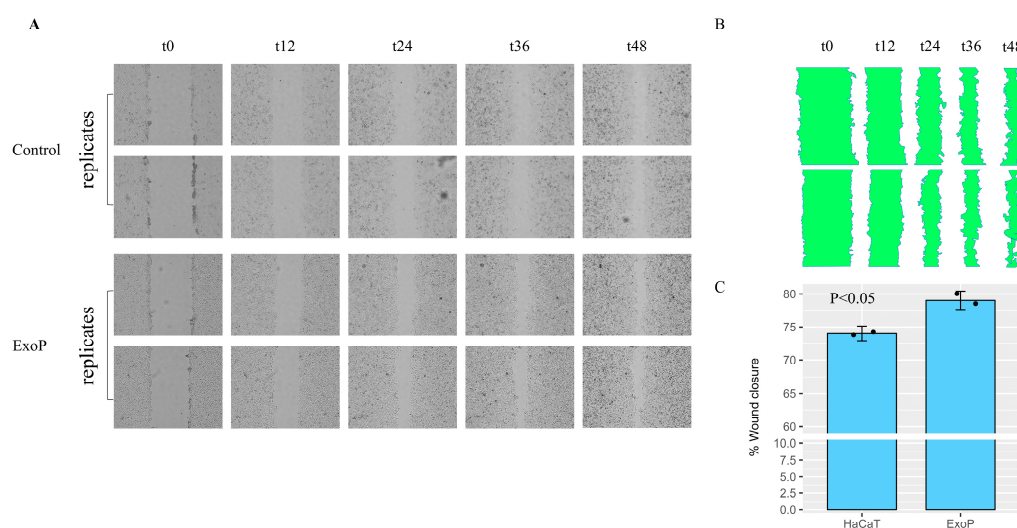


**Figure 2.** Facilitation of wound healing by SDEs. (A) HaCaT cells were subjected to a scratch at time zero (t0) and subsequently treated with either 1X PBS (Control) or SDEs in 1X PBS in duplicates. Photographs were captured at 12, 24, 36, and 48 h following the exosome treatment. (B) Areas of wounds at each observation location were delineated. A representative of the duplicates is shown. (C) The percentages of wound closure at t48 relative to t0 (refer to Methods) for 'Control' and 'SDEs' were illustrated as a bar graph, and the differences were analyzed using a two-sample t-test with the assumption of equal variances.

### 2.3. Impact of SDEs on the Expression of Genes Associated with the Skin Barrier

To assess the potential impact of SDEs on skin health, we examined the expression of various skin-related genes in keratinocyte HaCaT cells and fibroblast Detroit 551 cells following SDE treatment using RT-PCR, followed by analysis through agarose gel electrophoresis (Figure 3A). Our prior research demonstrated that SDEs at a concentration of 50  $\mu\text{g}/\text{mL}$  upregulated the expression of the antioxidant enzyme *GSTA4* in HaCaT keratinocytes. This effect can also be replicated in fibroblast Detroit 551 cells, indicating that SDEs may enhance antioxidant defenses across different cell types. Additionally, we observed that the expression of *FLG*, which aggregates keratin filaments into dense bundles to strengthen the cellular barrier, increased significantly due to SDE treatment at 50  $\mu\text{g}/\text{mL}$ , showing increases of 3.4-fold in HaCaT cells and 1.9-fold in Detroit 551 cells. Furthermore, *TGM1*, essential for epidermal barrier function, was significantly upregulated by 13 folds in HaCaT cells after SDE treatment; however, RT-PCR for *TGM1* in Detroit 551 fibroblasts was unsuccessful (Figure 3A). SDE treatment also induced hyaluronic acid synthase (HAS) genes in both keratinocytes and fibroblasts to varying extents. *HAS2* exhibited over 10-fold upregulation in both cell lines, while *HAS1* and *HAS3* showed greater upregulation in fibroblasts—exceeding 9 and 13 folds respectively—compared to more modest increases of over 2 and 4 folds in keratinocytes following SDE treatment. Notably, *AQP3* expression increased dramatically by at least 12,000% (or a 120-fold upregulation) in HaCaT cells after potato-derived exosomes treatment, indicating a significant enhancement in potential skin hydration capabilities; conversely, *AQP3* induction in Detroit 551 fibroblasts was more modest at a 2.6-fold increase. Additionally, SDE administration resulted in *KLK5* upregulation by over 4 folds in keratinocytes and over 8 folds in fibroblast cell lines. Collectively, these findings suggest that SDEs offer benefits to skin cells by strengthening the skin barrier, increasing hydration, regulating cell turnover, and protecting against environmental attacks, contributing to improved skin health.

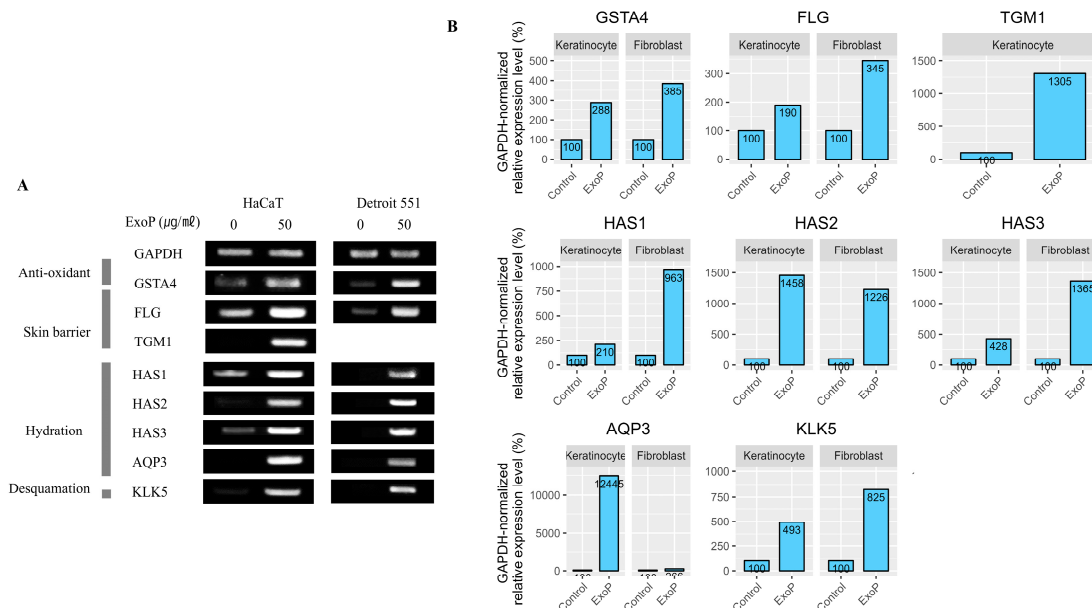


**Figure 3.** RT-PCR analysis of alterations in the expression of skin barrier genes in keratinocyte HaCaT and fibroblast Detroit 551 cells. (A) An agarose gel electrophoretic analysis of changes in gene expression levels of housekeeping gene *GAPDH* and skin barrier genes in both keratinocyte HaCaT and fibroblast Detroit 551 cells following treatment with potato-derived exosomes at a final concentration of 50  $\mu\text{g}/\text{mL}$ . (B) Agarose gel electrophoretic bands from (A) were analyzed for intensities using Image J (version 2; National Institute of Health) and subsequently plotted with the ggpubr package in R 4.3.1 for Windows and RStudio Version: 2023.06.0+421; <http://www.rstudio.com/>.

#### 2.4. Clinical Skin Assessment with Prototype Cosmetics Featuring SDEs as the Primary Component

The primary finding from this skin assessment was that no adverse reactions, such as redness, edema, scaling, itching, pain, or burning sensations, were observed in any participants after initial application and throughout the subsequent two-week duration (Table 1). Results demonstrated a significant cooling effect across all patients, with a maximum improvement of 16.04%, and minimum and median rates of 6.82% and 12.96%, respectively (Figure 4A and 4D). A statistically significant reduction in the depth of deep wrinkles around eyes was noted among all subjects, with improvements ranging from 4.76 to 25.74%, highlighting the effectiveness of SDEs in wrinkle reduction (Figure 4B and 4E). Moreover, the application of prototype cosmetics containing SDEs considerably enhanced skin elasticity (Figure 4G). Notably, a decrease in melanin levels was observed after two weeks of topical administration of SDE-containing prototypes, indicating potential benefits for pigmentation issues; this difference was statistically significant. In summary, these findings suggest that SDEs can provide substantial benefits for skin health by enhancing cooling effects, reducing wrinkles, improving elasticity, and reducing pigmentation levels.

**Table 1.** Skin adverse reaction.

Skin adverse reaction	N=21 (No. 01-02, 04-22)	
	After one-time use	After 2 weeks
1. Erythema (redness)	0	0
2. Edema (swelling)	0	0
3. Squama (keratin)	0	0
4. Itching	0	0
5. Tingling sensations (pain)	0	0
6. Burning sensation	0	0
7. Stiffness	0	0
8. Tingling	0	0

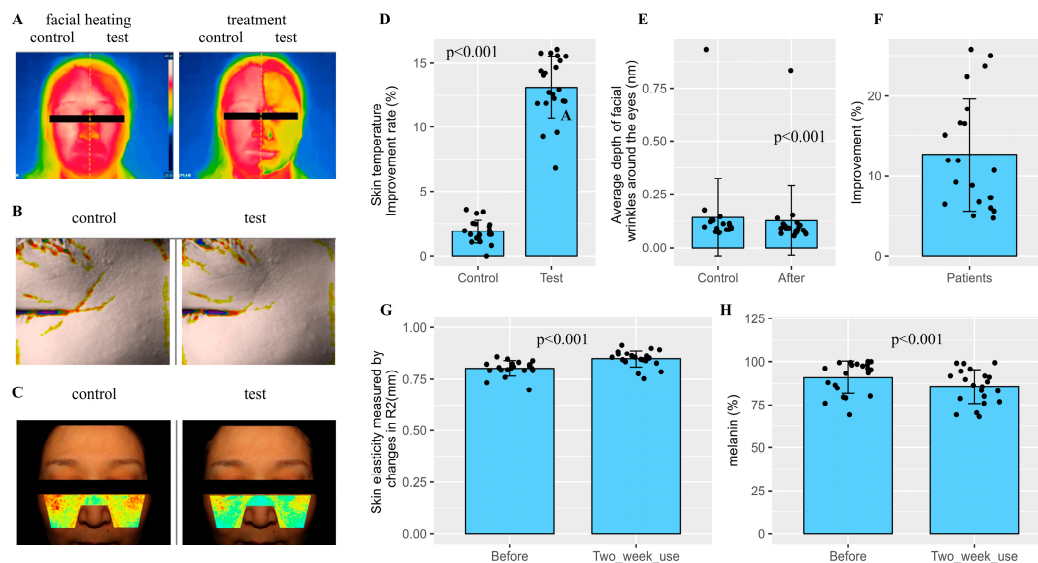


**Figure 4.** Clinical evaluations of the efficacy of cosmetic prototypes featuring SDEs as the primary component. (A) Representative images illustrating the immediate skin cooling effect. The left side presents a comparison between facial heating and cosmetic treatments devoid of potato-derived exosomes. The right side presents a comparison of facial heating and therapy using cosmetics that feature potato-derived exosomes as the primary ingredient. (B) Representative images of the anti-wrinkle impact. Deep wrinkles surrounding the eyes were evaluated before (left) and after (right) the use of cosmetics with SDEs as the primary ingredient. (C) Representative images illustrating the impact on melanin levels. (D) Improvements in skin cooling as a percentage of temperature changes after topical applications of cosmetic prototypes are shown for 21 volunteers. (E) Alterations in the profundity of deep eye wrinkles following topical applications of cosmetic prototypes are calculated. Relative enhancements in wrinkle depth (F), skin elasticity (G), and melanin content (H) were assessed in twenty-one subjects after the application of topical cosmetic prototypes.

### 3. Discussion

Our prior research demonstrated that SDEs exhibit significant anti-photoaging effects by inhibiting the expression of *MMP 1, 2, and 9*, as well as anti-inflammatory effects through the repression of cytokines *TNF* and *IL-6*, while enhancing the expression of antioxidant *GSTA4*. This study further investigates the skin-enhancing properties of SDEs by assessing their impact on wound healing and on the expression of skin barrier genes critical for skin health.

TNF, a key mediator of cutaneous inflammation, is linked to impaired skin barrier function in conditions like psoriasis, where diminished expression of epidermal barrier genes such as *FLG* is observed. TNF influences skin barrier gene expression through a signaling pathway involving the TNF receptor and c-Jun N-terminal kinase (JNK). The potential for SDEs to modulate skin barrier gene expression via the TNF-JNK signaling pathway will be investigated.

Together with previous data showing SDEs suppress *MMPs*, current *in vitro* studies suggest that SDEs may enhance skin hydration and strengthen barrier functions by upregulating skin barrier genes such as *FLG, TGM1, HASs, AQP3, and KLK5*, contributing to overall skin health while reducing UVB damage and wrinkles. A clinical skin test utilizing a formulation with SDEs as a major ingredient revealed no adverse responses while demonstrating effective anti-wrinkle benefits, improved skin elasticity, and reduction in pigmentation issues, providing a good starting point for evaluating SDEs in human applications, either for beauty or medical purposes.

To further elucidate the mechanisms underlying these observations, we are currently conducting comprehensive RNA-Seq analyses of messenger RNAs from SDE-treated HaCaT cells and small RNAs of the SDEs themselves. These ongoing studies promise to offer a more detailed

understanding of exosome composition and their impact on gene expression in HaCaT cells, complementing and extending our present findings.

Of the data presented, we are most interested in the safety results of SDEs on cell lines (Figure 1C) and the human skin test. Even with their high potential, no exosome-based commercial therapeutics have met the FDA's standards for safety and efficacy to date. The efficient cell permeability, combined with their safety profile, high-efficiency yield, and molecular delivery capacity (data not shown) may position these *Solanum tuberosum*-derived exosomes (SDEs) as a valuable resource to build on for potential applications in the medical and beauty industries.

Albeit at a small sample size, a clinical skin test utilizing a formulation with SDEs as a major ingredient revealed no adverse responses while demonstrating effective anti-wrinkle benefits, improved skin elasticity, and reduction in pigmentation issues. In conclusion, SDEs are safe and effective for cosmetic use on human skin, particularly in reducing deep eye wrinkles.

## 4. Materials and Methods

### 4.1. Reagents

Detroit 551 human fibroblast cells (cat. no. 10110) were purchased from Korean Cell Line Bank (Seoul, Republic of Korea). Keratinocyte HaCaT cells (cat. no. 300493) were purchased from CLS Cell Lines Service GmbH. Fetal bovine serum (FBS, heat inactivated, cat. no. 12106C), 1X phosphate buffered saline (PBS, pH 6.8~7.5, cat. no. LB004-01), 100X penicillin-streptomycin (10,000 units/mL, 10,000 µg/mL, respectively, cat. no. LS 202-02), Trypsin-EDTA (cat. no. LS 015-01), Minimum Essential Medium Eagle (MEM, cat. no. LM007-01), and Dulbecco's Modified Eagle's Medium (DMEM, cat. no. LM 001-07) were procured from WELGENE Inc (Gyeongsangbuk-do, Republic of Korea). Superscript II (catalog number 18064022) and Pierce™ Coomassie (Bradford) Protein Assay Kit (catalog number 23200) were procured from Thermo Fisher (Waltham, MS, USA). The Cell Proliferation Reagent WST-1 (catalog number 5015944001) was procured from Sigma-Aldrich (Burlington, MA, USA). The RNeasy Mini Kit (catalog number 74004) was obtained from Qiagen GmbH, located in Hilden, Germany. Oligonucleotide PCR primers were procured from Bionics in Seoul, Republic of Korea.

### 4.2. Preparation and Characterization of SDEs

The extraction of SDEs using ultracentrifugation and their size and morphology assessed using a Litesizer DLS 500 (Anton Paar, Austria) with dynamic light scattering, along with morphology assessment via transmission electron microscopy (TEM), were detailed in previous works [19]. After ultracentrifugation, the exosome preparations were subjected to filtration via 0.2 µm sterile filters to eliminate biological contaminants.

### 4.3. Cell Culture and SDE Administration

Keratinocyte HaCaT cells and fibroblast Detroit 551 were cultured in DMEM at a density of  $5 \times 10^3$  cells per well in a 96-well plate, supplemented with 10% FBS and final doses of 100 Units/mL of penicillin and 100 µg/mL of streptomycin, at 37 °C and 5% CO<sub>2</sub>. For the cell proliferation assay, SDEs were administered at a final concentration of 50 µg/mL and incubated for an additional 24 h prior to the application of the Cell Proliferation Reagent WST-1. Formazan production was observed at 420 nm using a microplate reader.

### 4.4. Reverse Transcription-Polymerase Chain Reaction (RT-PCR)

Total RNAs were extracted from HaCaT cells with the RNeasy mini kit. A reaction mixture of 13.4 µL, comprising 1 µg of total RNAs and 0.5 µg of oligo-dT primers, was incubated at 65 °C for 10 min. Superscript II (400 U), DTT, and dNTPs were incorporated into a final volume of 20 µL and incubated at 42 °C for 90 min. The MiniAmp Plus PCR equipment (Thermo Fisher) was employed for gene-specific amplifications, which involved an initial denaturation at 95 °C for 5 min, followed by

30 cycles of denaturation at 94 °C for 30 sec, annealing at 48 °C for 30 sec, and extension at 72 °C for 60 sec, concluding with a final incubation at 72 °C for 10 min. The oligonucleotide primer sets utilized for RT-PCR are enumerated in Table 2.

**Table 2.** Forward and reverse primer sequences for RT-PCR. Size (bp) refers to the size of the PCR products in base pairs.

Symbol	Name	size (bp)	Primer (5' → 3')
GAPDH	glyceraldehyde 3-phosphate dehydrogenase	380	ATTCCATGGCACCCTCAAGG
			TGATGGCATGGACTGTGGTC
GSTA4	glutathione S-transferase alpha 4	332	GAGGGGACACTGGATCTGCT
			GGAGGCTTCTTCTTGCTGCC
FLG	filaggrin	458	AGTGAGGCATACCCAGAGGA
			CCAAACGCACCTTGCTTTACA
TGM1	transglutaminase1	413	AATCCTCTGATCGCATCACC
			GTGGTCAAACCTGGCCGTAGT
HAS1	hyaluronan synthase 1	459	ACTCGGACACAAGGTTGGAC
			TGTACAGCCACTCACGGAAG
HAS2	hyaluronan synthase 2	463	TTTGGGTGTGTTTCAGTGCAT
			TAAGGCAGCTGGCAAAAGAT
HAS3	hyaluronan synthase 3	493	AGAAACCCGTGACCACTGAC
			ACCATCGAGATGCTTCGAGT
AQP3	aquaporin 3	427	CACACGATAAGGGAGGCTGT
			CCCTCATCTGGTGATGTTT
KLK5	kallikrein related peptidase 5	554	TGTGACCACCCCTCTAACAC
			TCCTCGCACCTTTTCTGACT

#### 4.5. Wound Healing Evaluations

HaCaT cells were seeded at a density of  $5 \times 10^5$  cells per well in 6-well plates containing DMEM supplemented with 10% FBS, along with final concentrations of 100 Units/mL of penicillin and 100 µg/mL of streptomycin. The cells were incubated for 24 h at 37 °C in a 5% CO<sub>2</sub> atmosphere, after which an artificial scratch was created using 200 µL pipette tips, and the cells were subsequently washed three times with 1X PBS. SDEs were subsequently included at a final concentration of 50 µg/mL. The JuLI™ Stage Real-Time Cell History Recorder was utilized to collect live cell imaging at time points 0, 12, 24, 36, and 48 h post SDEs addition. The percentages of wound closure were computed as follows, where  $t_0$  denotes the time at which the wound was inflicted, while  $t_n$  indicates the period after the addition of SDEs.

$$\text{Percentage of wound closure} = \frac{(\text{Wound surface area})_{t_0} - (\text{Wound surface area})_{t_n}}{(\text{Wound surface area})_{t_0}}$$

#### 4.6. Dermatological Clinical Assessment

A clinical study was conducted from April 3 to April 17, 2023, at Human Co., Ltd. Skin Clinical Trial Center (Seoul, Republic of Korea), with a study code of HE-P23-0066, in which written informed consent was obtained from all participants, to assess the efficacy of SDEs for immediate skin cooling effects after a single application, as well as improvements in skin elasticity, melasma, pigmentation, and facial wrinkles around the eyes after two weeks of use. The study was conducted in compliance with Good Clinical Practice (GCP) guidelines and the regulations set forth by the Ministry of Food and Drug Safety (MFDS) of the Republic of Korea and the standard operating procedures (SOP) of Human Co., Ltd. Skin Clinical Trial Center, Seoul, Republic of Korea. The alterations in periorbital wrinkles were evaluated for facial wrinkles. The study involved 21 healthy Korean male and female volunteers aged over 19 years, who were not on any medication or using cosmetics containing aspirin, anti-inflammatory agents, or antihistamines. Participants exhibiting diminished skin elasticity, pronounced periorbital wrinkles, and significant melasma and pigmentation were

incorporated into the test group. The prototype cosmetics used in this trial contained SDEs at a final concentration of 100 µg/mL and were applied once on the test day and twice daily, in the morning and evening, over a period of two weeks. The study aimed to assess the immediate cooling impact with a single application of a specific cosmetic, as well as the enhancement of skin elasticity, reduction of melasma and pigmentation, and alleviation of periorbital wrinkles after two weeks of usage. Assessments and measurements conducted in the climate-controlled chamber following a 30 min rest time. The room maintained an ambient temperature of  $22 \pm 2$  °C, with relative humidity of  $50 \pm 5\%$ . The skin cooling effects were assessed by comparing the skin surface temperatures (°C) of both cheeks prior to and following facial heating, as well as after a single application of the test product. Furthermore, the R2 (mm) and melanin percentage (%) of the cheek area were assessed both prior to and following a 2-week application of the test product to evaluate enhancements in skin elasticity, melasma, and pigmentation. Additionally, the average depth of wrinkles around one eye was analyzed to determine the product's effectiveness in reducing facial wrinkles in that region. The FLIR E75 Thermal Imaging Camera (FLIR Systems, Inc., Sweden) was utilized to assess the immediate cooling effect on the skin. The Cutometer® Dual MPA 580 was employed to assess variations in skin elasticity. DermaVision (Opto Biomed Co., Ltd., Republic of Korea) was utilized to assess the alterations in the levels of amelioration of melasma and pigmentation. The Antera 3D Camera for Skin Analysis (Miravex Ltd., Ireland) was employed to assess alterations in the degree of facial wrinkles surrounding the eyes. Antera 3D (Miravex Ltd., Ireland) is a device that analyzes skin by capturing images through reflections of seven distinct light wavelengths, utilizing a multi-spectral LED within the camera, in contrast to conventional imaging technologies that rely solely on three colors (RGB). A 3D image can be generated by optical techniques and intricate mathematical algorithms, facilitating accurate assessment of skin texture, fine lines, wrinkles, melanin levels, and hemoglobin levels.

**Declaration of Competing Interest:** RW Mohamed declares no competing interest. Y Lee is an employee, and S Yang serves as the CEO of Nextab, Inc.

**Author Contributions:** YeJI Lee: Conceptualization, Methodology, Formal analysis, Investigation, Data Curation, Formal analysis, Writing -review. Radwa Wahid Mohamed: Conceptualization, Writing -review. Sanghwa Yang: Conceptualization, Resource allocation, Visualization, Oversight, Formal analysis, Writing - review and editing. All authors have reviewed and consented to the published version of the work.

**Funding:** This research was funded by Korea Technology and Information Promotion Agency. for SMEs(TIPA) RS-2024-00511294 of Republic of Korea.

## References

1. Kim, D.J.; Iwasaki, A.; Chien, A.L.; Kang, S. UVB-Mediated DNA Damage Induces Matrix Metalloproteinases to Promote Photoaging in an AhR- and SP1-Dependent Manner. *JCI Insight* **2022**, *7*(9):e156344.
2. Brenneisen, P.; Sies, H.; Scharffetter-Kochanek, K. Ultraviolet-B Irradiation and Matrix Metalloproteinases: From Induction via Signaling to Initial Events. *Ann N Y Acad Sci* **2002**, *973*:31-43.
3. Candi, E.; Schmidt, R.; Melino, G. The Cornified Envelope: A Model of Cell Death in the Skin. *Nat Rev Mol Cell Biol* **2005**, *6*(4):328-340.
4. Montero-Vilchez, T.; Segura-Fernández-nogueras, M.V.; Pérez-Rodríguez, I.; Soler-Gongora, M.; Martínez-Lopez, A.; Fernández-González, A.; Molina-Leyva, A.; Arias-Santiago, S. Skin Barrier Function in Psoriasis and Atopic Dermatitis: Transepidermal Water Loss and Temperature as Useful Tools to Assess Disease Severity. *J Clin Med* **2021**, *10*(2):359.

5. Kim, B.E.; Howell, M.D.; Guttman, E.; Gilleaudeau, P.M.; Cardinale, I.R.; Boguniewicz, M.; Krueger, J.G.; Leung, D.Y.M. TNF- $\alpha$  Downregulates Filaggrin and Loricrin through c-Jun N-Terminal Kinase: Role for TNF- $\alpha$  Antagonists to Improve Skin Barrier. *J Invest Dermatol.* **2011**, *131*(6):1272-1279.
6. Wikramanayake, T.C.; Stojadinovic, O.; Tomic-Canic, M. Epidermal Differentiation in Barrier Maintenance and Wound Healing. *Adv Wound Care (New Rochelle)* **2014**, *3*(3):272-280.
7. Wilkins, R.G.; Unverdorben, M. Wound Cleaning and Wound Healing: A Concise Review. *Adv Skin Wound Care* **2013**, *26*(4):160-163
8. Rezaie, J.; Feghhi, M.; Etemadi, T. A Review on Exosomes Application in Clinical Trials: Perspective, Questions, and Challenges. *Cell Commun Signal.* **2022**, *20*(1):145.
9. Alvarez-Erviti, L.; Seow, Y.; Yin, H.; Betts, C.; Lakkhal, S.; Wood, M.J.A. Delivery of SiRNA to the Mouse Brain by Systemic Injection of Targeted Exosomes. *Nat Biotechnol* **2011**, *29*(4):341-345.
10. Matsumoto, J.; Stewart, T.; Sheng, L.; Li, N.; Bullock, K.; Song, N.; Shi, M.; Banks, W.A.; Zhang, J. Transmission of  $\alpha$ -Synuclein-Containing Erythrocyte-Derived Extracellular Vesicles across the Blood-Brain Barrier via Adsorptive Mediated Transcytosis: Another Mechanism for Initiation and Progression of Parkinson's Disease? *Acta Neuropathol Commun* **2017**, *5*(1):71.
11. Banks, W.A.; Sharma, P.; Bullock, K.M.; Hansen, K.M.; Ludwig, N.; Whiteside, T.L. Transport of Extracellular Vesicles across the Blood-Brain Barrier: Brain Pharmacokinetics and Effects of Inflammation. *Int J Mol Sci* **2020**, *21*(12):4407.
12. Tenchov, R.; Sasso, J.M.; Wang, X.; Liaw, W.S.; Chen, C.A.; Zhou, Q.A. Exosomes Nature's Lipid Nanoparticles, a Rising Star in Drug Delivery and Diagnostics. *ACS Nano* **2022**, *16*(11):17802-17846.
13. Zhang, Y.; Liu, Q.; Zhang, X.; Huang, H.; Tang, S.; Chai, Y.; Xu, Z.; Li, M.; Chen, X.; Liu, J.; Yang C. Recent Advances in Exosome-Mediated Nucleic Acid Delivery for Cancer Therapy. *J Nanobiotechnology* **2022**, *20*(1):279.
14. Mu, J.; Zhuang, X.; Wang, Q.; Jiang, H.; Deng, Z. Bin; Wang, B.; Zhang, L.; Kakar, S.; Jun, Y.; Miller, D.; et al. Interspecies Communication between Plant and Mouse Gut Host Cells through Edible Plant Derived Exosome-like Nanoparticles. *Mol Nutr Food Res* **2014**, *58*(7):1561-1573.
15. Dad, H.A.; Gu, T.W.; Zhu, A.Q.; Huang, L.Q.; Peng, L.H. Plant Exosome-like Nanovesicles: Emerging Therapeutics and Drug Delivery Nanoplatfoms. *Mol Ther* **2021**, *29*(1):13-31.
16. Yi, Q.; Xu, Z.; Thakur, A.; Zhang, K.; Liang, Q.; Liu, Y.; Yan, Y. Current Understanding of Plant-Derived Exosome-like Nanoparticles in Regulating the Inflammatory Response and Immune System Microenvironment. *Pharmacol Res* **2023**, *190*:106733.
17. Arif, S.; Larochele, S.; Trudel, B.; Gounou, C.; Bordeleau, F.; Brisson, A.R.; Moulin, V.J. The Diffusion of Normal Skin Wound Myofibroblast-derived Microvesicles Differs According to Matrix Composition. *J Extracell Biol* **2023**, *3*(1):e131.
18. Faria-Silva, C.; Ascenso, A.; Costa, A.M.; Marto, J.; Carvalheiro, M.; Ribeiro, H.M.; Simões, S. Feeding the Skin: A New Trend in Food and Cosmetics Convergence. *Trends Food Sci Technol* **2020**, *95*, 21–32.
19. Lee, Y.; Jeong, D.-Y.; Jeun, Y.C.; Choe, H.; Yang, S. Preventive and Ameliorative Effects of Potato Exosomes on UVB-induced Photodamage in Keratinocyte HaCaT Cells. *Mol Med Rep* **2023**, *28*(3):167.
20. Ashcroft, G.S.; Jeong, M.J.; Ashworth, J.J.; Hardman, M.; Jin, W.; Moutsopoulos, N.; Wild, T.; McCartney-Francis, N.; Sim, D.; McGrady, G.; et al. Tumor Necrosis Factor-Alpha (TNF- $\alpha$ ) Is a Therapeutic Target for Impaired Cutaneous Wound Healing. *Wound Repair Regen* **2012**, *20*(1):38-49.
21. Bhat, B.B.; Kamath, P.P.; Chatterjee, S.; Bhattacharjee, R.; Nayak, U.Y. Recent Updates on Nanocosmeceutical Skin Care and Anti-Aging Products. *Curr Pharm Des* **2022**, *28*(15):1258-1271.

22. Verbavatz, J.M.; Boury-Jamot, M.; Daraspe, J.; Bonté, F.; Perrier, E.; Schnebert, S.; Dumas, M. Skin Aquaporins: Function in Hydration, Wound Healing, and Skin Epidermis Homeostasis. *Handb Exp Pharmacol* **2009**, *190*, 205–217.
23. Bollag, W.B.; Aitkens, L.; White, J.; Hyndman, K.A. Aquaporin-3 in the Epidermis: More than Skin Deep. *Am J Physiol Cell Physiol* **2020**, *18(6)*:C1144-C1153.
24. Drislane C.; Irvine AD. The Role of Filaggrin in Atopic Dermatitis and Allergic Disease. *Ann Allergy Asthma Immunol.* **2020**, *124(1)*:36-43.
25. Yang, J.M.; Ahn, K.S.; Cho, M.O.; Yoneda, K.; Lee, C.H.; Lee, J.H.; Lee, E.S.; Candi, E.; Melino, G.; Ahvazi, B.; et al. Novel Mutations of the Transglutaminase 1 Gene in Lamellar Ichthyosis. *J Invest Dermatol* **2001**, *117(2)*:214-218.
26. Caubet, C.; Jonca, N.; Brattsand, M.; Guerrin, M.; Bernard, D.; Schmidt, R.; Egelrud, T.; Simon, M.; Serre, G. Degradation of Corneodesmosome Proteins by Two Serine Proteases of the Kallikrein Family, SCTE/KLK5/HK5 and SCCE/KLK7/HK7. *J Invest Dermatol.* **2004**, *122(5)*:1235-1244.
27. Milstone, L.M. Epidermal Desquamation. *J Dermatol Sci* **2004**, *36(3)*:131-140.
28. Nauroy, P.; Nyström A. Kallikreins: Essential Epidermal Messengers for Regulation of the Skin Microenvironment during Homeostasis, Repair and Disease. *Matrix Biol Plus* **2019** *21*:6-7:100019.
29. Göllner, I.; Voss, W.; von Hehn, U.; Kammerer, S. Ingestion of an Oral Hyaluronan Solution Improves Skin Hydration, Wrinkle Reduction, Elasticity, and Skin Roughness: Results of a Clinical Study. *J Evid Based Complementary Altern Med* **2017**, *22*.
30. Li, H.; Guo, H.; Lei, C.; Liu, L.; Xu, L.; Feng, Y.; Ke, J.; Fang, W.; Song, H.; Xu, C. and Yu, C. Nanotherapy in joints: increasing endogenous hyaluronan production by delivering hyaluronan synthase 2. *Adv Mater* **2019**, *31(46)*:e1904535
31. Sayo, T.; Sugiyama, Y.; Takahashi, Y.; Ozawa, N.; Sakai, S.; Ishikawa, O.; Tamura, M.; Inoue, S. Hyaluronan Synthase 3 Regulates Hyaluronan Synthesis in Cultured Human Keratinocytes. *J Invest Dermatol* **2002**, *118(1)*:43-8.

**Disclaimer/Publisher's Note:** The statements, opinions and data contained in all publications are solely those of the individual author(s) and contributor(s) and not of MDPI and/or the editor(s). MDPI and/or the editor(s) disclaim responsibility for any injury to people or property resulting from any ideas, methods, instructions or products referred to in the content.